Journal of Organometallic Chemistry, *469* (1994) 33–40

Transition metal Schiff-base complexes as ligands in tin chemistry

IV. Reactions of triphenyltin chloride with divalent metal salicylaldimine complexes and the molecular structures of [$SnPh_3Cl \cdot H_2O$]–[Ni(3-MeOsal1,3pn) · H_2O] (1 : 1) and [$SnPh_3Cl \cdot H_2O$]–Ni(3-MeOsal1,3pren) (1 : 1) [$H_2$3-MeOsal1,3pn = *N*,*N*′-bis(3-methoxysalicylidene)propane-1,3-diamine]

N. Clarke, D. Cunningham, T. Higgins, P. McArdle, J. McGinley and M. O'Gara

Department of Chemistry, University College Galway, Galway (Ireland)

(Received August 11, 1993)

Abstract

Unlike diorganotin(IV) dihalides, triphenyl- and tribenzyl-tin chlorides do not react with Schiff-base complexes M(SB) (M = Cu^{II}, Ni^{II} and Zn^{II}; SB = *N*,*N*′-ethylenebis-salicylideneaminato and related salicylaldimine ligands). Triphenyltin chloride does however form 1 : 1 addition complexes with 3,3′-methoxy substituted salicylaldimines of Ni^{II} and Cu^{II}, but only in the presence of water. Each of these complexes contains the aquo adduct $SnPh_3Cl \cdot H_2O$, with the donor water molecule engaged in hydrogen bonding interactions with the four oxygen atoms of the divalent metal salicyaldimine. These structural features were confirmed crystallographically for ($SnPh_3Cl \cdot H_2O$)–Ni(3-MeOsal1,3pn) (1 : 1) [$H_2$3-MeOsal1,3pn = *N*,*N*′-bis(3-methoxysalicylidene)propane-1,3-diamine]. In the case of [$SnPh_3Cl \cdot H_2O$]–[Ni(3-MeOsal1,3pn) · H_2O] (1 : 1) both the water molecule coordinated to nickel and the water molecule coordinated to tin engage in hydrogen bonding interactions with the Schiff-base oxygen atoms, thereby creating centrosymmetric hydrogen-bonded dimers.

Key words: Tin; Mössbauer spectroscopy

1. Introduction

Previous studies have shown that nickel(II), copper(II), and cobalt(II) salicylaldimines are very effective neutral chelating donor ligands for tin(II) halides, tin(IV) halides, and both mono- and diorganotin(IV) halides [1–7]. Crystallographic studies of $SnMe_2Cl_2 \cdot$ Ni(salen) and $Sn^nBuCl_2(OMe) \cdot$ CoCl (salen) [H_2salen = *N*,*N*′-bis(salicylidene)ethylenediamine] have confirmed the engagement of both phenolic oxygens of the salicylaldimine ligand in donor bond formation (in anisobidentate fashion) to tin [6,7]. The presence of methoxy substituents in the 3,3′ positions of the metal salicylaldimine ligands markedly alters the nature of the addition complexes that they form with diorganotin(IV) Lewis acids. Two general types of complexes result. When the bridging group linking the salicylaldimine nitrogen atoms is a two-carbon atom bridge, aquo adducts of the diorganotin(IV) species are formed, with the donor water molecule held to the metal salicylaldimine complex by hydrogen bonding interactions, as shown schematically in Fig. 1(a) [8]. When the bridging group contains three or four carbon atoms, diorganotin cations $(SnR_2)^{2+}$ or $(SnR_2X)^+$ (X = halogen or pseudohalogen) are generated, the tin atom of which in all cases lies in the plane of, and engages in donor bond formation with, the four Schiff-base oxygen atoms, as shown in Figs. 1(b) and (c) [9]. When the groups X migrate from tin to the transition

---

Correspondence to: Professor D. Cunningham.

0022-328X/94/$7.00
SSDI 0022-328X(93)24123-M

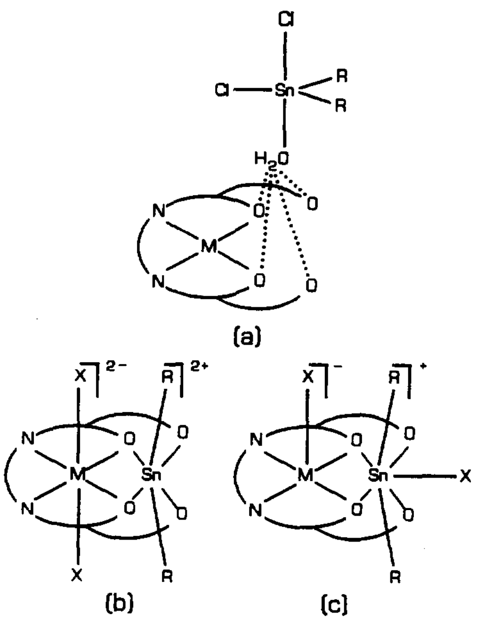

Fig. 1. Schematic representation of the structures of the adducts from the reactions of SnR_2X_2 (R = organo group; X = halide, thiocyanate, or nitrate) with divalent metal (M) 3-methoxysalicylaldiimine complexes. Dotted lines signify hydrogen bonding interactions.

metal, as indicated in Figs. 1(b) and (c), novel examples of intimate ion-paired heterobimetallic complexes are formed. In view of this diverse reactivity if diorganotin Lewis acids with metal salicylaldimine complexes, we decided to investigate the analogous reactions with triorganotin species. The present paper describes the reactions of triphenyl- and tribenzyl-tin chlorides with divalent metal salicylaldimine complexes, and discusses the structures (as deduced from infrared and ^{119}Sn Mössbauer spectroscopic and crystallographic studies) of 1:1 addition complexes resulting from such reactions.

2. Results and discussion

Although diorganotin(IV) dihalides and dithiocyanates readily react with nickel, copper, and cobalt, and in some cases zinc, salicylaldimine complexes to yield 1:1 addition compounds [2–6,9], this is not the case with triphenyl- and tribenzyltin tin(IV) chlorides (see Experimental section). The inability of triphenyltin chloride to form adducts with the metal salicylaldimine complexes is somewhat surprising in view of the large range of Lewis acids, including alkali and alkaline earth metal cations [10], which have been shown to coordinate to the metal salicylaldimines in question.

The situation is rather different when the salicylaldimine ligands have methoxy substituents in the 3,3′ positions. Triphenyltin chloride readily formed 1:1 addition complexes with divalent metal methoxysalicylaldimines when the metal was copper or nickel, but not when it was zinc. The Lewis acidity of triphenyltin chloride under these circumstances apparently comes close to the limiting value necessary for complexation to the metal salicylaldimine hydrates, since tribenzyltin chloride failed to react with any of them.

A significant feature of the reactions which resulted in adduct formation was that in each case the presence of water was required. This was strikingly demonstrated by the fact that the anhydrous complexes M(3-MeOsal1,3pn) ($M = Ni^{II}$ or Cu^{II}) did not react with triphenyltin chloride under rigorously moisture-free conditions. In view of the fact that triphenyltin chloride is apparently incapable of forming donor bonds with either the phenolic or methoxy oxygens, and that the presence of water was required for adduct formation, there is the strong suggestion that the 1:1 addition complexes of this study are aquo adducts of triphenyltin chloride, similar to those of dimethyltin dichloride that are shown schematically in Fig. 1(a). Further support for the aquo adduct type structure of Fig. 1(a) comes from key features of the infrared spectra of the complexes, and it is confirmed by X-ray crystallographic studies for both $[SnPh_3Cl \cdot H_2O]$–Ni(3-MeOsal1,3pn) (1 : 1) and $[SnPh_3Cl \cdot H_2O]$–[Ni(3-MeOsal1,3pn)$\cdot H_2O$] (1:1) The inability of triphenyltin chloride to form an aquo adduct with the water molecule of the zinc methoxyalicylaldimine hydrates is somewhat surprising. However, dimethyltin dichloride did not form donor bonds with the water molecules of the zinc complexes in question, opting instead to form donor bonds with Schiff-base oxygen atoms [9].

The asymmetric units of $[SnPh_3Cl \cdot H_2O]$–Ni(3-MeOsal1,3pn) (1:1) (**A**) and $[SnPh_3Cl \cdot H_2O]$–[Ni(3-MeOsal1,3pn)$\cdot H_2O$] (1:1) (**B**) (see Figs. 2 and 3, respectively) reveal that the complexes have the same fundamental structure, each containing the adduct $SnPh_3Cl \cdot H_2O$ with the donor water molecule engaged in hydrogen bonding to the Schiff-base oxygen atoms. They differ in that in **A** the aquo adduct is hydrogen bonded to an approximately square planar low-spin nickel salicylaldimine complex, whereas in **B** it is hydrogen bonded to a square pyramidal high-spin nickel salicylaldimine complex, the square pyramidal geometry being a consequence of the second water molecule forming a donor bond to nickel. The presence of this second donor water molecule introduces some interesting contrasts in the structures, not only because it results in a change of the spin state of nickel, but also because it engages in hydrogen bonding interactions with the Schiff-base oxygen atoms of a neighbouring molecule, thus producing the hydrogen bonded dimer shown in Fig. 4. The hydrogen bonded dimeric core,

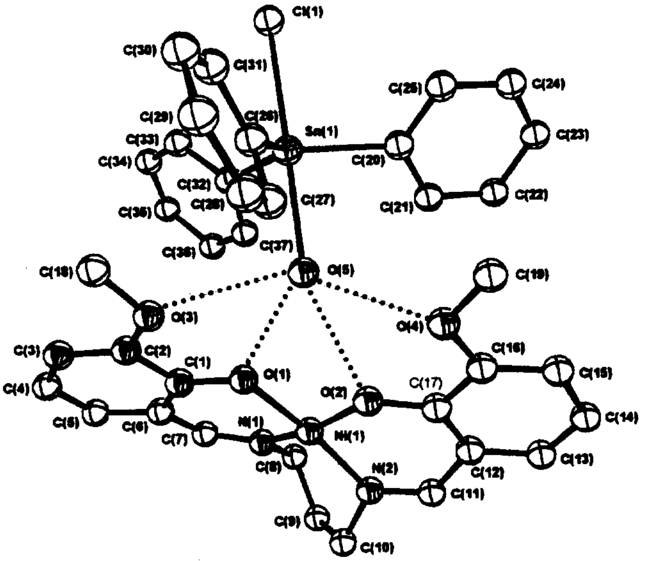

Fig. 2. The asymmetric unit of A. Dotted lines signify hydrogen bonding interactions.

$[Ni(3\text{-}MeOsal1,3pn) \cdot H_2O]_2$, of this structure is similar to that present in the structure of the parent nickel salicylaldimine [9], and, for example, in the structure of $Co(3\text{-}MeOsalen) \cdot H_2O$ [11].

Similar trigonal bipyramidal tin coordination geometry is present in the aquo adduct of A and B. In each case, the tin is slightly out of the equatorial plane, defined by three carbon atoms bonded to it, towards the axial chlorine, thus giving rise to Cl–Sn–C bond angles somewhat greater than the O–Sn–C bond angles (see Tables 1 and 2). The discrepancy between the magnitudes of the two sets of angles is somewhat less in the aquo adduct having the stronger Sn–O bond (i.e. in A). While the axial O–Sn–Cl bond angles differ by only 0.6° there is a significant difference in the Sn–O bond lengths, B having a Sn–O bond length of 2.420(3) Å and A a Sn–O bond length of 2.334(4) Å. The difference in Sn–Cl bond lengths (approximately 0.02 Å) is less pronounced, with the shorter Sn–Cl bond associated with the longer Sn–O bond.

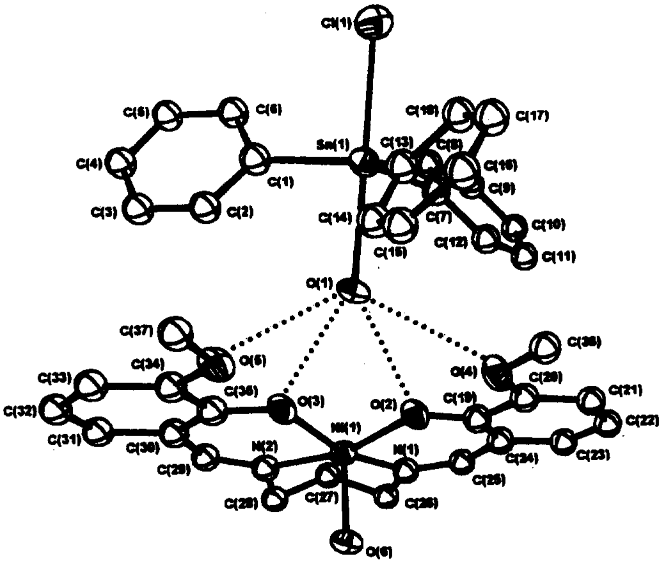

Fig. 3. The asymmetric unit of B. Dotted lines signify hydrogen bonding interactions.

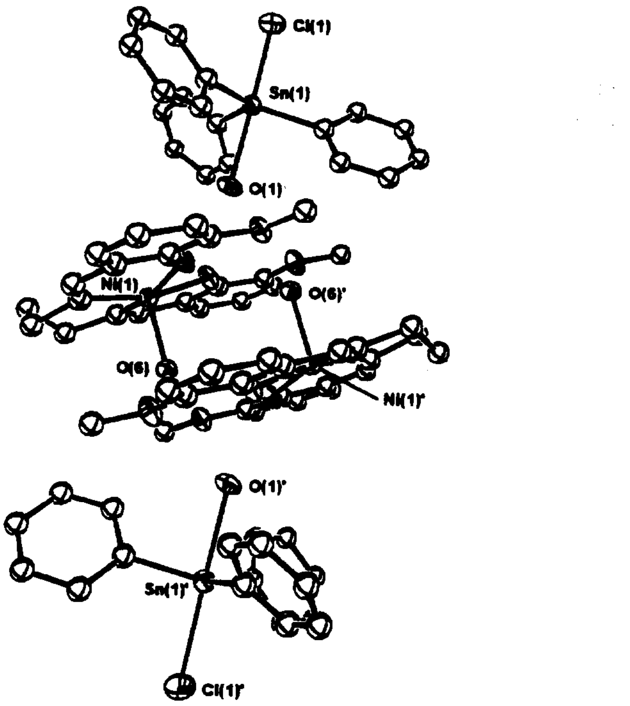

Fig. 4. Dimerization of B through hydrogen bonding interactions (see Discussion).

The phenolic oxygen and imine nitrogen bond lengths to nickel are typical of those found for high-spin and low-spin nickel salicylaldimines complexes, with the substantially longer bond lengths associated with high-spin nickel (in B). In the case of the high-spin complex B, the phenolic oxygen and imine nitrogen atoms define good planar geometry, with the nickel ion removed from the mean square plane defined by these atoms by 0.168 Å towards the water molecule. The overall conformation of the salicylaldimine ligand in this complex comes close to planar. In the case of the diamagnetic complex A, the coordination geometry about nickel displays a distinct tetrahedral distortion, such that the planes defined by Ni, O(1) and N(1) (plane A) and Ni, O(2) and N(2) (plane B) are inclined to each other at an angle of 14.413°. The irregular conformation of the salicylaldimine ligand in this complex (see Fig. 5), being typical of that which we have found in many low-spin nickel salicylaldimnie complexes having a 1,3-propylene bridge, results in the six-membered ring comprising nickel, imine nitrogens, and propylene carbon atoms adopting a boat conformation; this contrasts with the chair, or half-chair, conformation associated with high-spin nickel complexes. (These structural features will be discussed in more detail in a future paper.) The main point to be stressed therefore is that the substantial differences in ligand conformation which are apparent in the present complexes are more related to the nickel spin state than to the nature of the hydrogen bonding interaction that are described below.

In the case of **A**, the distances between the water oxygen and Schiff-base oxygens range from 2.76 to 2.97 Å, so that hydrogen bonding interactions appear to involve all four Schiff-base oxygens (in neither this structure, nor that of **B**, were the hydrogen atoms of the water molecules located). The average distance between the water oxygens and Schiff-base oxygens of 2.85 Å compares with very similar distances of 2.83 and 2.85 Å for the structurally related adducts $[SnMe_2Cl_2 \cdot H_2O]$–Ni(3-MeOsalen) (1 : 1) and $[SnMe_2Cl_2 \cdot H_2O]$–Ni(3-MeOsal1,2pn) (1 : 1), respectively [8].

TABLE 1. Selected bond lengths (Å) and angles (°) in **A**

Sn(1)–Cl(1)	2.508(2)	Sn(1)–O(5)	2.333(4)
Sn(1)–C(20)	2.134(6)	Sn(1)–C(26)	2.137(6)
Sn(1)–C(32)	2.130(6)	Ni(1)–O(1)	1.876(4)
Ni(1)–O(2)	1.853(3)	Ni(1)–N(1)	1.868(4)
Ni(1)–N(2)	1.1871 (4)	O(1)–C(1)	1.331(7)
O(2)–C(17)	1.316(6)	O(3)–C(2)	1.375(8)
O(3)–C(18)	1.417(8)	O(4)–C(16)	1.385(7)
O(4)–C(19)	1.434(7)	N(1)–C(7)	1.298(8)
N(1)–C(8)	1.480(8)	N(2)–C(10)	1.476(7)
N(2)–C(11)	1.295(7)	C(1)–C(2)	1.422(9)
C(1)–C(6)	1.422(8)	C(2)–C(3)	1.358(9)
C(3)–C(4)	1.41(1)	C(4)–C(5)	1.33(1)
C(5)–C(6)	1.43(1)	C(6)–C(7)	1.412(9)
C(8)–C(9)	1.490(9)	C(9)–C(10)	1.540(8)
C(11)–C(12)	1.430(7)	C(12)–C(13)	1.395(9)
C(12)–C(17)	1.416(7)	C(13)–C(14)	1.332(9)
C(14)–C(15)	1.45(1)	C(15)–C(16)	1.376(9)
C(16)–C(17)	1.419(7)		

O(5)–Sn(1)–Cl(1)	178.7(1)	C(12)–C(17)–O(2)	124.8(5)
C(20)–Sn(1)–O(5)	87.1(2)	C(20)–Sn(1)–Cl(1)	93.5(2)
C(26)–Sn(1)–O(5)	87.1(2)	C(26)–Sn(1)–Cl(1)	93.7(2)
C(32)–Sn(1)–Cl(1)	93.1(2)	C(26)–Sn(1)–C(20)	115.2(2)
C(32)–Sn(1)–C(20)	117.0(2)	C(32)–Sn(1)–O(5)	85.6(2)
O(2)–Ni(1)–O(1)	85.0(2)	C(32)–Sn(1)–C(26)	126.7(2)
N(1)–Ni(1)–O(2)	168.7(2)	N(1)–Ni(1)–O(1)	93.4(2)
N(2)–Ni(1)–O(2)	93.2(2)	N(2)–Ni(1)–O(1)	169.7(2)
C(1)–O(1)–Ni(1)	125.8(4)	N(2)–Ni(1)–N(1)	90.4(2)
C(18)–O(3)–C(2)	116.0(5)	C(17)–O(2)–Ni(1)	126.2(3)
C(7)–N(1)–Ni(1)	125.3(4)	C(19)–O(4)–C(16)	116.4(5)
C(8)–N(1)–C(7)	117.0(5)	C(8)–N(1)–Ni(1)	117.6(4)
C(11)–N(2)–Ni(1)	126.5(4)	C(10)–N(2)–Ni(1)	116.8(4)
C(2)–C(1)–O(1)	120.0(5)	C(11)–N(2)–C(10)	116.1(5)
C(6)–C(1)–C(2)	117.1(5)	C(6)–C(1)–O(1)	122.9(5)
C(3)–C(2)–O(3)	124.7(6)	C(1)–C(2)–O(3)	113.7(5)
C(7)–C(6)–C(1)	121.1(6)	C(7)–C(6)–C(5)	118.7(7)
C(6)–C(7)–N(1)	126.6(6)	C(9)–C(8)–N(1)	111.9(5)
C(10)–C(9)–C(8)	112.5(6)	C(9)–C(10)–N(2)	111.9(5)
C(12)–C(11)–N(2)	125.1(5)	C(13)–C(12)–C(11)	119.4(5)
C(17)–C(12)–C(11)	119.9(5)	C(15)–C(16)–O(4)	123.3(6)
C(17)–C(16)–O(4)	113.6(5)	C(16)–C(17)–O(2)	118.8(5)

TABLE 2. Selected bond lengths (Å) and angles (°) in **B**

Sn(1)–Cl(1)	2.482(1)	Sn(1)–O(1)	2.418(2)
Sn(1)–C(1)	2.126(3)	Sn(1)–C(7)	2.135(3)
Sn(1)–C(13)	2.139(3)	Ni(1)–O(2)	2.011(2)
Ni(1)–O(3)	1.986(2)	Ni(1)–O(6)	2.025(2)
Ni(1)–N(1)	2.050(3)	Ni(1)–N(2)	2.057(3)
O(2)–C(19)	1.319(4)	O(3)–C(35)	1.316(4)
O(4)–C(20)	1.376(5)	O(4)–C(36)	1.423(4)
O(5)–C(34)	1.365(4)	O(5)–C(37)	1.409(5)
N(1)–C(25)	1.293(5)	N(1)–C(26)	1.470(5)
N(2)–C(28)	1.489(5)	N(2)–C(29)	1.288(5)
C(19)–C(20)	1.410(5)	C(19)–C(24)	1.410(5)
C(20)–C(21)	1.366(5)	C(21)–C(22)	1.399(6)
C(22)–C(23)	1.366(7)	C(23)–C(24)	1.419(5)
C(24)–C(25)	1.417(6)	C(26)–C(27)	1.467(8)
C(27)–C(28)	1.498(8)	C(29)–C(30)	1.433(5)
C(30)–C(31)	1.411(5)	C(30)–C(35)	1.410(5)
C(31)–C(32)	1.348(6)	C(32)–C(33)	1.392(6)
C(33)–C(34)	1.376(5)	C(34)–C(35)	1.409(5)

O(1)–Sn(1)–Cl(1)	179.2(1)	C(1)–Sn(1)–Cl(1)	95.8(1)
C(1)–Sn(1)–O(1)	84.6(1)	C(7)–Sn(1)–Cl(1)	94.0(1)
C(7)–Sn(1)–O(1)	85.2(1)	C(7)–Sn(1)–C(1)	117.9(1)
C(13)–Sn(1)–Cl(1)	95.7(1)	C(13)–Sn(1)–O(1)	84.7(1)
C(13)–Sn(1)–C(1)	116.3(1)	C(13)–Sn(1)–C(7)	123.4(1)
O(3)–Ni(1)–O(2)	83.0(1)	O(6)–Ni(1)–O(2)	98.5(1)
O(6)–Ni(1)–O(3)	98.3(1)	N(1)–Ni(1)–O(2)	88.8(1)
N(1)–Ni(1)–O(3)	165.5(1)	N(1)–Ni(1)–O(6)	94.7(1)
N(2)–Ni(1)–O(2)	165.2(1)	N(2)–Ni(1)–O(3)	89.4(1)
N(2)–Ni(1)–O(6)	95.2(1)	N(2)–Ni(1)–N(1)	95.8(1)
C(19)–O(2)–Ni(1)	129.0(2)	C(35)–O(3)–Ni(1)	129.2(2)
C(36)–O(4)–C(20)	118.2(3)	C(37)–O(5)–C(34)	118.6(3)
C(25)–N(1)–Ni(1)	124.8(3)	C(26)–N(1)–Ni(1)	119.5(3)
C(26)–N(1)–C(25)	115.5(4)	C(28)–N(2)–Ni(1)	121.5(3)
C(29)–N(2)–Ni(1)	124.5(2)	C(29)–N(2)–C(28)	113.8(3)
C(20–C(19)–O(2)	119.5(3)	C(24)–C(19)–O(2)	123.2(3)
C(21)–C(20)–O(4)	123.9(4)	C(19)–C(20)–O(4)	113.9(3)
C(25)–C(24)–C(19)	123.2(3)	C(25)–C(24)–C(23)	117.3(4)
C(24)–C(25)–N(1)	128.9(3)	C(27)–C(26)–N(1)	114.2(4)
C(28)–C(27)–C(26)	114.9(5)	C(27)–C(28)–N(2)	112.1(4)
C(30)–C(29)–N(2)	128.8(3)	C(31)–C(30)–C(29)	117.9(3)
C(35)–C(30)–C(29)	122.2(3)	C(33)–C(34)–O(5)	124.7(3)
C(35)–C(34)–O(5)	113.8(3)	C(34)–C(35)–O(3)	118.5(3)
C(30)–C(35)–O(3)	124.3(3)		

The distances between the water oxygens and Schiff-base oxygens within the dimeric core, $[Ni(3\text{-}MeOsal1,3\text{-}pn) \cdot H_2O]_2$ of **B** are very similar to those in Co(3-MeOsalen) · H_2O [11]. For example, distances of 2.83 and 2.86 Å from the water oxygen to the methoxy oxygens, and 2.94 and 2.96 Å to the phenolic oxygens for **B** compare with distances of 2.97 Å from the water oxygen to methoxy oxygens, and 2.85 Å to the phenolic oxygens for the cobalt salicylaldimine. The essential

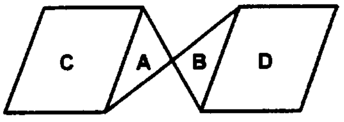

PLANE(S)	ATOMS IN PLANE
A	Ni(1), N(1) and O(1)
B	Ni(1), N(2) and O(2)
C	N(1), O(1) and C(1) - C(7)
D	N(2), O(2) and C(11) - C(17)

ANGLE BETWEEN PLANES (°)	
A and C	18.863
A and B	14.413
B and D	17.006
C and D	15.286

Fig. 5. Conformational geometry of Ni(3-MeOsal1,3pn) in A.

difference between the hydrogen bonding in the two complexes is that, in **B**, the strongest interactions are with the methoxy oxygens, whereas in the case of the cobalt complex they are with the phenolic oxygens.

As a result of the strong hydrogen bonding interactions within the dimeric core, the involvement of the water oxygen of the aquo adduct $SnPh_3Cl \cdot H_2O$ in hydrogen bonding interactions differs markedly in the structures of **A** and **B**. In the case of **B**, the water oxygen to phenolic oxygen distances of 2.75 and 2.76 Å suggest strong hydrogen bonding interactions, while the distances of 3.36 and 3.43 Å to the methoxy oxygens are suggestive of either very weak or no hydrogen bonding interactions. Thus, the strong hydrogen bonding interactions, not surprisingly, are with the oxygens that are associated with the weaker interactions within the dimeric core. Finally, a comparison of the hydrogen bonding interactions for **A** and **B** reveals that the water molecule of $SnPh_3Cl \cdot H_2O$ which is more extensively involved in hydrogen bonding interactions (in **A**) also forms the stronger Sn–O bond, and this is consistent with earlier observations [8].

We have previously shown that the position of the infrared bands above 3000 cm^{-1}, which are associated with water involved in hydrogen bonding with the oxygen atoms of divalent methoxysalicylaldimine complexes, move to significantly lower frequencies when the water also becomes involved in donor bond formation [8]. Formation of the donor bond also results in a small increase in the phenolic ν(C–O) stretching frequency; we have attributed this increase to a strengthening of hydrogen bonding interactions accompanying donor bond formation. In the case of the first five complexes of Table 3, the characteristic frequency shifts described above are clearly apparent, and these observations, coupled with the observation that water is necessary for adduct formation, establish beyond reasonable doubt that the complexes are isostructural with **A**. The position of the water-associated band in the spectrum of $SnPh_3Cl \cdot H_2O]$–Cu(3-MeOsal1,3pn) (1 : 1) is also consistent with the aquo adduct structure. (The position of the band cannot, in this case, be compared with that for the parent copper salicylaldimine since this was isolated as an anhydrous complex).

The complex Ni(3-MeOsal1,3pn) · H_2O differs from the other nickel salicylaldimines of this study in that the water not only engages in hydrogen bonding but also forms an intermolecular donor bond with nickel. Consequently, the position of the water-related band above 3000 cm^{-1} for this complex is at a significantly lower frequency than observed for the other salicylaldimine complexes (see Table 3). Furthermore, since the dual bonding role of water in Ni(3-MeOsal1,3pn) · H_2O is maintained in **A**, it is not surprising that the position of this water-related infrared band remains relatively unchanged on formation of **A** (see Table 3), nor is it particularly surprising that, despite the presence of two different water environments in **B**, only one water-associated band is observed in the high region of its infrared spectrum.

TABLE 3. Selected infrared and ^{119}Sn Mössbauer spectroscopic data [a]

Complex	ν(O–H) (cm^{-1})	ν(C–O) (cm^{-1})	δ (mm s^{-1})	Δ (mm s^{-1})
($SnPh_3Cl \cdot H_2O$)–Ni(3-MeOsalen) (1 : 1)	3357 (3515)	1548 (1540)	1.34	3.20
($SnPh_3Cl \cdot H_2O$)–Ni(3-MeOsal1,2pn) (1 : 1)	3360 (3500, 3450)	1549 (1546)	1.36	3.14
($SnPh_3Cl \cdot H_2O$)–Ni(3-MeOsalphen) (1 : 1)	3390 (3470)	1540 (1535)	1.37	3.17
($SnPh_3Cl \cdot H_2O$)–Cu(3-MeOsalen) (1 : 1)	3352 (3505, 3461)	1547 (1544)	1.30	3.23
($SnPh_3Cl \cdot H_2O$)–Cu(3-MeOsal1,2pn) (1 : 1)	3366 (3477)	1547 (1536)	1.29	3.07
($SnPh_3Cl \cdot H_2O$)–Cu(3-MeOsal1,2pn) (1 : 1)	3374 (none)	1551 (1538)	1.29	3.17
($SnPh_3Cl \cdot H_2O$)–Ni(3-MeOsal1,3pn) (1 : 1)	3380 (3370)	1547 (1547)	1.34	3.16
($SnPh_3Cl \cdot H_2O$)–[Ni(3-MeOsal1,3pn) · H_2O] (1 : 1)	3386 (3370)	1553 (1547)	1.32	2.80

[a] δ ±0.03 mm s^{-1}; Δ ±0.05 mm s^{-1}.

The Mössbauer parameters in Table 3 reveal that for six of the eight complexes the quadrupole splitting values lie within the range 3.14–3.23 mm s^{-1}, *i.e.* the variations are within the range of experimental error. The smallest quadrupole splittings of 2.80 and 3.07 mm s^{-1} were observed for **B** and $SnPh_3Cl \cdot H_2O$–Cu(3-MeOsal1,2pn) (1 : 1), respectively. The constancy of the quadrupole splitting data for the majority of the complexes points to a marked similarity in the tin coordination geometry, which of course is not unexpected in view of the fact that they each contain the aquo adduct $SnPh_3Cl \cdot H_2O$. The striking difference in the aquo adducts contained in **A** and **B** lies in the significantly longer Sn–O donor bond in **B**, which, in turn, results in a greater displacement of tin from the equatorial plane towards the axial chlorine atom, and it is obviously these structural differences that account for the difference in quadrupole splittings for the complexes. This observation leads to the suggestion that the aquo adduct in $SnPh_3Cl$–Cu(3-MeOsal1,2pn) (1 : 1) contains a somewhat weaker Sn–O donor bond than those present in the majority of the adducts.

3. Experimental details

IR spectra were recorded on a Perkin-Elmer 983G spectrometer. Details of the Mössbauer spectrometer and of the Mössbauer spectra curve fitting routine have been described elsewhere [4]. Triphenyltin chloride (Aldrich) was used without further purification. Tribenzyltin chloride was prepared by reaction of tin powder with benzyl chloride, and was recrystallized from ethyl acetate. Divalent metal salicylaldimine complexes were prepared by published methods [12].

3.1. Reactions of triphenyl- and tribenzyl-tin(IV) chloride with divalent metal salicylaldimine complexes

Typically, 0.01 mol of the tin Lewis acid was added to an equimolar quantity of the divalent metal in *ca.* 100 cm^3 of either chloroform or acetonitrile (both solvents were used for each reaction). The mixture was stirred for 3 h at room temperature and the solid then filtered off and dried under a vacuum. In those instances in which 1 : 1 adduct formation took place, reactions were repeated with twice the mole quantity of the tin Lewis acid, but in no case did this alter the 1 : 1 composition of the adducts.

Neither triphenyl- nor tribenzyl-tin chloride reacted with M(salen) [M = Ni^{II}, Cu^{II} or Zn^{II}; H_2salen = *N*,*N*′-bis(salicylidene)rthylenediamine], M(salphen) [M = Ni^{II}, Cu^{II} or Zn^{II}; H_2salphen = *N*,*N*′-bis(salicylidene)-*o*-phenylenediamine], M(sal1,2pn) [M = Ni^{II}, Cu^{II} or Zn^{II}; H_2sal1,2pn = *N*,*N*′-bis(salicylidene) propane-1,2-diamine], or M(α-Me-salen) [M = Ni^{II}, Cu^{II} or Zn^{II}; $H_2\alpha$-Me-salen = *N*,*N*′-bis(α-methylsalicylidene)ethylenediamine].

Triphenyltin chloride formed 1 : 1 addition complexes with M(3-MeOsalen) · H_2O [M = Ni^{II} or Cu^{II}; $H_2$3-MeOsalen = *N*,*N*′-bis(3-methoxysalicylidene)ethylenediamine], M(3-MeOsalphen) · H_2O [M = Ni^{II} or Cu; $H_2$3-MeOsalphen = *N*,*N*′-bis(3-methoxysalicylidene)-*o*-phenylenediamine], M(3-MeOsal1,2pn) · H_2O [M = Ni^{II} or Cu^{II}; $H_2$3-MeOsal1,2pn = *N*,*N*′-bis(3-methoxysalicylidene)propane-1,2-diamine], Ni(3-MeOsal1,3pn) · H_2O and Cu(3-MeOsal1,3-pn) [$H_2$3-MeOsal1,3pn = *N*,*N*′-bis(3-methoxysalicylidene)propane-1,3-diamine]. It did not react with the zinc analogues of the above complexes, and tribenzyltin chloride reacted with none of the complexes. Analytical data are given in Table 4.

TABLE 4. Analytical data for the adducts [a]

	C	N	H	Cl
($SnPh_3Cl \cdot H_2O$)–Ni(3-MeOsalen) (1 : 1)	55.11	4.44	4.63	4.63
	(54.67)	(3.54)	(4.43)	(4.49)
($SnPh_3Cl \cdot H_2O$)–Ni(3-MeOsal1,2pn) (1 : 1)	55.29	3.45	4.86	4.23
	(55.21)	(3.48)	(4.60)	(4.41)
($SnPh_3Cl \cdot H_2O$)–Ni(3-MeOsalphen) (1 : 1)	57.34	3.45	4.22	4.11
	(57.40)	(3.35)	(4.19)	(4.25)
($SnPh_3Cl \cdot H_2O$)–Cu(3-MeOsalen) (1 : 1)	54.73	3.52	4.38	5.03
	(54.53)	(3.53)	(4.42)	(4.48)
($SnPh_3Cl \cdot H_2O$)–Cu(3-MeOsal1,2pn) (1 : 1)	54.95	3.31	4.59	4.92
	(55.07)	(3.47)	(4.59)	(4.40)
($SnPh_3Cl \cdot H_2O$)–Cu(3-MeOsal1,3pn) (1 : 1)	55.13	3.53	4.80	5.02
	(55.02)	(3.47)	(4.59)	(4.40)
($SnPh_3Cl \cdot H_2O$)–Ni(3-MeOsal1,3pn) (1 : 1)	54.71	3.26	4.97	4.26
	(55.21)	(3.48)	(4.69)	(4.41)
($SnPh_3Cl \cdot H_2O$)–[Ni(3-MeOsal1,3pn) · H_2O] (1 : 1)	54.31	3.52	4.88	4.10
	(54.16)	(3.41)	(4.79)	(4.32)

[a] Theoretical data are in parentheses.

Whereas the reaction of triphenyltin chloride with Ni(3-MeOsal1,3pn)·H_2O in acetonitrile yielded, almost immediately, a green paramagnetic solid **A**, the reaction in chloroform, with a triphenyltin chloride/nickel salicylaldimine mole ratio of 2:1, yielded a brownish-red diamagnetic crystalline complex **A** when the solvent was reduced to approximately half its volume and set aside for several days. One of the crystals was suitable for a crystallographic study. Good quality crystals of the paramagnetic adduct were obtained when a hot saturated acetonitrile solution was allowed to cool over a period of *ca.* 24 h.

3.2. Reactions of triphenyltin(IV) chloride with Ni(3-MeOsal1,3pn) and Cu(3-MeOsal1,3pn) under anhydrous conditions

The complex Ni(3-MeOsal1,3pn)·H_2O was dehydrated either by stirring the monohydrate in acetone for 3h (resulting in a colour change of the precipitate from green to brown) or by heating it under a vacuum at 100°C for 2 h. Ni(3-MeOsal1,3pn) (0.01 mol) was treated with triphenyltin chloride (0.01 mol) in acetonitrile under strictly moisture-free conditions for 6 h, after which the starting materials were recovered. Similar results were obtained when acetone and chloroform were used as solvents, and also when the reactions were conducted under reflux. However, when moisture-free conditions were not rigorously maintained, the adduct [SnPh$_3$Cl · H_2O]–[Ni(3-MeOsal1,3pn) · H_2O] (1:1) was slowly formed. It was found that under moisture-free conditions, triphenyltin chloride also failed to react with Cu(3-MeOsal1,3pn).

TABLE 5. Crystallographic details

	A	**B**
Formula	$C_{37}H_{37}N_2ClO_5NiSn$	$C_{37}H_{39}N_2ClO_6NiSn$
M (a.m.u.)	802.553	820.568
Space group	P_{21}/n (monoclinic)	$\bar{P}$ (triclinic)
a (Å)	11.350(1)	12.298(1)
b (Å)	21.301(3)	12.553(1)
c (Å)	14.657(2)	13.021(1)
α (°)	90.0	94.0(2)
β (°)	100.18(2)	116.0(2)
γ (°)	90.0	103.2(2)
U (Å^3)	3487.76	1726.17
Z	4	2
D_c (g cm^3)	1.528	1.579
$F(000)$	1632	836
Crystal dimensions (mm)	0.3×0.2×0.25	0.32×0.28×0.41
μ(Mo Kα) (cm^{-1})	12.78	12.94
Data collected	$\pm h$ $+k$ $+l$	$\pm h$ $\pm k$ $+l$
Unique reflections	6996	8888
Reflections with $I > 3\sigma(I)$	5357	7059
No. of parameters	252	100
R^b (%)	6.51	4.12
R'^c	8.18	4.86
g^c	0.00124	0.00012
Max. shift (e.s.d.)	0.001	0.001
Residual density max (min) (e Å^{-3})	0.59 (−0.45)	0.64 (−0.38)
Goodness of fit ^{d}	0.97	1.443

[a] All measurements performed at 20°C on a CAD4 diffractometer with graphite-monochromated Mo Kα radiation ($\lambda = 0.71069$ Å), scan range $2 < \theta < 24°$. Scan method ω–2θ. [b] $R = [\Sigma \| F_o| - |F_c \|]/\Sigma |F_o|$. [c] $R' = \{[\Sigma w(|F_o - F_c|)^2]/[\Sigma w(|F_o|)^2]\}^{1/2}$; $w = 1/[(\sigma F_o)^2 - gF_o^2]$. [d] Goodness of fit $= [\Sigma w(|F_o| - |F_c|)^2/(N_{obs} - N_{parameters})]^{1/2}$.

TABLE 6. Fractional atomic coordinates for **A**

Atom	x	y	z
Sn(1)	0.08633(3)	0.21133(2)	0.55377(3)
Ni(1)	0.66227(5)	0.02174(3)	0.51514(4)
Cl(1)	0.91290(16)	0.28333(7)	0.55928(16)
O(1)	0.7129(3)	−0.0525(2)	0.5791(2)
O(2)	0.6176(3)	−0.0304(2)	0.4136(2)
O(3)	0.7267(4)	−0.1672(2)	0.6487(3)
O(4)	0.5967(4)	−0.1188(2)	0.2884(3)
O(5)	1.2451(4)	0.1432(2)	0.5458(3)
N(1)	0.7372(4)	0.0732(2)	0.6114(3)
N(2)	0.5842(4)	0.0915(2)	0.4546(3)
C(1)	0.7426(5)	−0.0584(3)	0.6707(4)
C(2)	0.7524(6)	−0.1192(3)	0.7117(4)
C(3)	0.7785(7)	−0.1268(4)	0.8050(5)
C(4)	0.8061(8)	−0.0741(4)	0.8633(6)
C(5)	0.8024(8)	−0.0160(4)	0.8292(6)
C(6)	0.7713(6)	−0.0063(3)	0.7312(4)
C(7)	0.7744(6)	0.0553(3)	0.6962(4)
C(8)	0.7638(5)	0.1387(3)	0.5880(4)
C(9)	0.6533(6)	0.1777(3)	0.5671(5)
C(10)	0.5460(5)	0.1409(3)	0.5137(4)
C(11)	0.5472(5)	0.0975(2)	0.3662(4)
C(12)	0.5559(5)	0.0501(3)	0.2985(4)
C(13)	0.5205(6)	0.0641(3)	0.2046(5)
C(14)	0.5173(6)	0.0212(3)	0.1380(5)
C(15)	0.5419(6)	−0.0439(3)	0.1632(5)
C(16)	0.5738(5)	−0.0582(3)	0.2557(4)
C(17)	0.5849(4)	−0.0123(2)	0.3270(3)
C(18)	0.7485(9)	−0.2288(4)	0.6844(6)
C(19)	0.5842(8)	−0.1676(3)	0.2200(5)
C(22)	1.1094(8)	0.0900(5)	0.7994(6)
C(23)	1.0846(10)	0.1319(6)	0.8679(9)
C(24)	1.0624(11)	0.1908(7)	0.8477(9)
C(25)	1.0660(8)	0.2153(4)	0.7598(7)
C(26)	1.2080(6)	0.2865(3)	0.5438(4)
C(27)	1.3318(6)	0.2775(3)	0.5629(5)
C(28)	1.4086(7)	0.3285(3)	0.5621(5)
C(29)	1.3692(7)	0.3874(4)	0.5433(6)
C(30)	1.2470(8)	0.3964(4)	0.5224(6)
C(31)	1.1658(7)	0.3478(4)	0.5256(5)
C(32)	0.9904(5)	0.1578(3)	0.4421(4)
C(33)	0.9018(6)	0.1845(4)	0.3763(5)
C(34)	0.8363(8)	0.1476(4)	0.3047(6)
C(35)	0.8552(9)	0.0865(4)	0.2996(7)
C(36)	0.9464(8)	0.0588(4)	0.3633(6)
C(37)	1.0115(6)	0.0936(3)	0.4358(5)

Table 7. Fractional atomic coordinates for **B**

Atom	*x*	*y*	*z*
Sn(1)	0.24052(2)	0.70626(2)	0.36054(2)
Ni(1)	0.22483(4)	0.09002(3)	0.11351(4)
Cl(1)	0.30462(11)	0.57600(9)	0.49562(9)
O(1)	0.1796(2)	0.8324(2)	0.2276(2)
O(2)	0.1688(2)	−0.0724(2)	0.0412(2)
O(3)	0.1287(2)	0.0349(2)	0.1977(2)
O(4)	0.0249(2)	−0.2755(2)	−0.0656(2)
O(5)	−0.0457(3)	−0.0697(2)	0.2452(2)
O(6)	0.0899(2)	0.1391(2)	−0.0147(2)
N(1)	0.3479(3)	0.1183(3)	0.0448(3)
N(2)	0.3034(3)	0.2412(2)	0.2265(3)
C(1)	0.3277(3)	0.8529(3)	0.4919(3)
C(2)	0.2592(4)	0.9269(3)	0.4937(3)
C(3)	0.3166(4)	1.0264(4)	0.5761(4)
C(4)	0.4430(4)	1.0495(4)	0.6586(4)
C(5)	0.5116(5)	0.9761(4)	0.6561(4)
C(6)	0.4543(4)	0.8787(4)	0.5733(4)
C(7)	0.3409(3)	0.6682(3)	0.2711(3)
C(8)	0.4587(4)	0.6498(3)	0.3334(3)
C(9)	0.5316(5)	0.6365(4)	0.2809(4)
C(10)	0.4888(4)	0.6404(4)	0.1645(4)
C(11)	0.3711(4)	0.6568(3)	0.1001(4)
C(12)	0.2997(4)	0.6706(3)	0.1536(3)
C(13)	0.0417(3)	0.6356(3)	0.2956(3)
C(14)	−0.0436(4)	0.6315(3)	0.1802(3)
C(15)	−0.1719(4)	0.5828(4)	0.1400(4)
C(16)	−0.2164(5)	0.5417(4)	0.2121(4)
C(17)	−0.1347(5)	0.5461(4)	0.3269(4)
C(18)	−0.0037(4)	0.5921(3)	−0.3683(4)
C(19)	0.1869(3)	−0.1205(3)	−0.0411(3)
C(20)	0.1138(3)	−0.2306(3)	−0.0998(3)
C(21)	0.1300(4)	−0.2855(4)	−0.1840(3)
C(22)	0.2212(5)	−0.2333(4)	−0.2153(4)
C(23)	0.2934(4)	−0.1264(4)	−0.1608(4)
C(24)	0.2780(4)	−0.0675(3)	−0.0735(3)
C(25)	0.3537(4)	0.0446(4)	−0.0256(4)
C(26)	0.4285(5)	0.2321(4)	0.0658(5)
C(27)	0.4855(5)	0.2931(5)	0.1859(6)
C(28)	0.3968(4)	0.3340(3)	0.2175(5)
C(29)	0.2728(3)	0.2674(3)	0.3056(3)
C(30)	0.1787(4)	0.2029(3)	0.3313(3)
C(31)	0.1520(4)	0.2558(3)	0.4130(3)
C(32)	0.0617(5)	0.2019(4)	0.4387(3)
C(33)	−0.0077(4)	0.0920(3)	0.3833(3)
C(34)	0.0169(3)	0.0376(3)	0.3040(3)
C(35)	0.1101(3)	0.0914(3)	0.2745(3)
C(36)	−0.0536(4)	−0.3865(3)	−0.1196(4)
C(37)	−0.1424(4)	−0.1310(4)	0.2666(4)

3.3. X-Ray crystallography

Crystallographic details for both [$SnPh_3Cl \cdot H_2O$]–Ni(3-MeOsal1,3pn) (1 : 1) and [$SnPh_3Cl \cdot H_2O$]–[Ni(3-Me)1,3pn) $\cdot$ H_2O] (1 : 1) are given in Table 5. The structures were solved by direct methods, SHELX86 [13], and refined by full matrix least-squares using SHELX 76 [14]. Data were corrected for Lorentz, polarization and extinction effects, but not for absorption. Hydrogen atoms were included in calculated positions for final refinement cycles. In the case of [$SnPh_3Cl \cdot H_2O$]–Ni(3-MeOsal1,3pn) (1 : 1), tin, nickel, chlorine, oxygen and nitrogen atoms were refined anisotropically, and in the case of [$SnPh_3Cl \cdot H_2O$]–[Ni(3-MeOsal1,3pn) $\cdot$ H_2O] (1 : 1) all atoms of the nickel salicylaldimine, oxygen atoms of the water molecules, chlorine and tin atoms were all refined anisotropically. The atomic scattering factors for all atoms, and the anomalous dispersion correction factors for non-hydrogen atoms were taken from the literature [15–17]. Calculations were carried out on a VAX 8700 computer. Final atomic coordinates are in Tables 6 and 7 The ORTEP [18] program was used to produce the drawings of Figs. 2–4. Complete lists of bond lengths and angles and table of thermal parameters and hydrogen atom coordinates have been deposited with the Cambridge Crystallographic Data Centre.

Acknowledgements

We are grateful to the Higher Education Authority for financial support to N.C.J. McG. and M. O'G.

References

1 M.D. Hobday and T.D. Smith, *J. Chem. Soc. A.*, (1971) 1453.
2 L. Pellerito, R. Cefalu, A. Gianguzza and R. Barbieri, *J. Organomet. Chem.*, *70* (1974) 303.
3 T.N. Strivastava, A.K.S. Chauhan and M. Agarval, *Transition Met. Chem.* (Weinheim), *3* (1978) 378.
4 D. Cunningham, J. Fitzgerald and M. Little, *J. Chem. Soc., Dalton Trans.*, (1987) 2261.
5 D. Cunningham and J. McGinley, *J. Chem., Soc., Dalton Trans.*, (1992) 1387.
6 M. Calligaris, L. Randaccio, R. Barbieri and L. Pellerito, *J. Organomet. Chem.*, *76* (1974) C57.
7 D. Cunningham, T. Higgins, B. Kneafsey, P. McArdle and J. Simmie, *J. Chem. Soc., Chem. Commun.*, (1985) 231.
8 D. Cunningham, J.F. Gallagher, T. Higgins, P. McArdle, J. McGinley and M. O'Gara, *J. Chem. Soc., Dalton Trans.*, (1993) 2183.
9 M. Boyce, D. Cunningham, J. McGinley and D. Sheerin, unpublished work.
10 See, for example, C. Floriani, M. Fiallo, A. Chiesi-Villa and C. Guastini, *J. Chem. Soc., Dalton Trans.*, (1987) 1367 and refs. therein.
11 M. Galligaris, G. Nardin and L. Randaccio, *J. Chem. Soc., Dalton Trans.*, (1974) 1903.
12 P.J. McCarthy, R.J. Hovey, K. Ueno and A.E. Martell, *J. Am. Chem., Soc.*, *77* (1955) 5820.
13 G.M. Sheldrick, SHELX 86, *Package for Crystal Structure Determination*, University of Göttingen, 1986.
14 G.M. Sheldrick, SHELX 76, *Package for Crystal Structure Determination*, University Cambridge, UK, 1976.
15 D.T. Cromer and J.B. Mann, *Acta Crystallogr., Sect. A*, *24* (1968) 321.
16 R.F. Stewart, E.R. Davidson and W.T. Simpson, *J. Chem. Phys.*, *42* (1965) 3175.
17 D.T. Cromer and D.J. Liberman, *J. Chem. Phys.*, *53* (1970) 1861.
18 C.K. Johnson, ORTEP, Report ORNL-3794, Oak Ridge National Laboratory, TN, 1971, pp. 1965–3794.